AWARD NUMBER: W81XWH-17-1-0455

TITLE: New Hydrocephalus Therapies Through Interruption of Lipid Signaling and Inflammatory Pathways Using Novel Drug-Like Compounds

PRINCIPAL INVESTIGATOR: Jerold Chun, MD, Ph.D.

CONTRACTING ORGANIZATION: Sanford Burnham Prebys Medical Discovery Institute
La Jolla, CA

REPORT DATE: June 2021

TYPE OF REPORT: Final Technical

PREPARED FOR: U.S. Army Medical Research and Development Command
Fort Detrick, Maryland 21702-5012

REPORT DOCUMENTATION PAGE

Form Approved
OMB No. 0704-0188

1. REPORT DATE	2. REPORT TYPE	3. DATES COVERED
June 2021	Final	01Sep2017 - 28Feb2021

4. TITLE AND SUBTITLE

New Hydrocephalus Therapies Through Interruption of Lipid Signaling and Inflammatory Pathways Using Novel Drug-Like Compounds

5a. CONTRACT NUMBER

5b. GRANT NUMBER
W81XWH-17-1-0455

5c. PROGRAM ELEMENT NUMBER

6. AUTHOR(S)

Jerold Chun, MD, Ph.D.

E-Mail: jchun@sbpdiscovery.org

5d. PROJECT NUMBER

5e. TASK NUMBER

5f. WORK UNIT NUMBER

7. PERFORMING ORGANIZATION NAME(S) AND ADDRESS(ES)

Sanford Burnham Prebys Medical Discovery Institute
10901 N. Torrey Pines Road
La Jolla, CA 92037-1005

8. PERFORMING ORGANIZATION REPORT NUMBER

9. SPONSORING / MONITORING AGENCY NAME(S) AND ADDRESS(ES)

U.S. Army Medical Research and Development Command
Fort Detrick, Maryland 21702-5012

10. SPONSOR/MONITOR'S ACRONYM(S)

11. SPONSOR/MONITOR'S REPORT NUMBER(S)

12. DISTRIBUTION / AVAILABILITY STATEMENT

Approved for Public Release; Distribution Unlimited

13. SUPPLEMENTARY NOTES

14. ABSTRACT

Lysophosphatidic acid (LPA) and its lipid precursor lysophosphatidylcholine (LPC) are abundant lipid molecules found in the blood and are released into the cerebral spinal fluid (CSF) during hemorrhage or traumatic events. Previous studies showed that when injected into the lateral ventricles of the fetal mouse brain, LPA produced hydrocephalus and associated brain morphological abnormalities. The purpose of this proposal is to develop and implement fetal and neonatal models of post hemorrhagic hydrocephalus (PHH) using the LPA lipid precursor LPC towards the pursuit of developing novel therapies for the prevention and treatment of post-traumatic hydrocephalus.

Key to achieving these goals, both Aims were essentially completed. LPC delivery into the lateral ventricles of neonatal mice was found to produce hydrocephalus with comparable neuropathologies to those produced by LPA. Histological changes were refractory to autotaxin (ATX) inhibition by the compound GWJ-23; however, survival curves were markedly improved, with behavioral endpoints trending towards at least partial utility for autotaxin inhibition in reducing PHH behavioral deficits and thus improving quality of life. Improved ATX inhibitor compounds should be assessed in the future. Neuroimmunological chemokines were increased in cerebral spinal fluid (CSF), suggesting a distinct mechanism of damage that could also be interrupted to provide therapeutic benefit in future PHH assessments.

15. SUBJECT TERMS

Post hemorrhagic hydrocephalus, Lysophosphatidyl choline, Lysophosphatidic acid

16. SECURITY CLASSIFICATION OF:			17. LIMITATION OF ABSTRACT	18. NUMBER OF PAGES	19a. NAME OF RESPONSIBLE PERSON
a. REPORT	b. ABSTRACT	c. THIS PAGE			USAMRDC
Unclassified	Unclassified	Unclassified	Unclassified	21	19b. TELEPHONE NUMBER *(include area code)*

Standard Form 298 (Rev. 8-98)
Prescribed by ANSI Std. Z39.18

TABLE OF CONTENTS

1. SUMMARY AND INTRODUCTION

Summary

This project focused on the roles of lysophosphatidic acid (LPA) and its precursor, lysophosphatidylcholine (LPC), in inducing post-hemorrhagic hydrocephalus (PHH), its associated neuropathology, and possible lysophospholipid-based therapeutic interventions. To examine the roles of LPA and LPC in PHH, we developed a mouse model to approximate a vulnerable stage in human perinatal development. *Aim 1* focused on determining the specific neuropathologies associated with PHH that are induced after LPA/LPC injection into the ventricles of postnatal day 8 (P8) mice. We characterized LPA/LPC-induced PHH neuropathologies and assessed the ability of agents that interfere with the LPA biosynthesis pathway, particularly autotaxin (ATX, which converts LPC to LPA *in vivo*). *Aim 2* was directed at understanding how neuroinflammation contributes to PHH neuropathology at the cellular and molecular levels. We used immunomodulators and pharmacological inhibitors of the LPA/LPC pathway to determine if exposing the mouse brain to these agents can ameliorate PHH.

Major Results

- Two doses of the ATX inhibitor (ATXi), GWJ-23, had no efficacy in preventing increased ventricular volume, ependymal cell loss, myelin defects, or macrophage infiltration assessed at P15 following 1 week of LPC exposure.
- Immunofluorescence staining of brain sections and staining of cleared whole brains using SWITCH showed corroborative histopathological changes associated with hydrocephalus in the LPC-injected brain.
- At later ages, GWJ-23 may partially reverse LPC-induced gait changes, deficits in grip strength, motor coordination, ambulation, exploratory behavior, as well as promote survival.
- Cerebrospinal fluid (CSF) derived from LPC-injected brains at P15 showed elevated levels of chemokines known to attract CD4+ T cells, neutrophils, and monocytes to the sites of pathological injury.
- The anti-inflammatory agents minocycline and dexamethasone were not effective in ameliorating the LPC-induced hydrocephalic effects assessed at P15.
- Combination therapy with GWJ-23 and minocycline also failed to reverse LPC-induced hydrocephalus assessed at P15.

Progress on Milestones

Aim 1.1: Test three ATXis to demonstrate efficacy in preventive and/or therapeutic cohorts: **100% complete**.

Aim 1.2: Complete motor and cognitive assessments of hydrocephalic mice and cohorts treated with ATXis in prevention and therapeutic paradigms: **100% complete**.

Aim 2.1: Complete assessment of neuroinflammation in LPC-induced PHH: **90% complete**.

Aim 2.2: Complete examination of neuroinflammatory modulation on PHH neuropathology and behavior while preparing manuscripts for publication, attending conferences to ensure data sharing, and assessing plans for future applications: **90% complete**.

Major Conclusions

- We developed a mouse model of PHH using intraventricular delivery of 5µl of 2.5mM LPC into the brains of P8 mice. The mice developed ventriculomegaly accompanied by histopathological and behavioral changes, and neuroinflammation.
- Blocking ATX-mediated LPA production using GWJ-23 did not prevent the LPC-induced PHH typically seen 1 week after LPC exposure at P15.
- Pre-treatment with GWJ-23 partially restored LPC-induced changes in gait (particularly stride length), as well as deficits in grip strength, motor coordination, ambulation, and exploratory behavior.
- Pre-treatment with GWJ-23 protected against LPC-associated mortality.
- Neuroinflammation was examined at 2 timepoints following induction of hydrocephalus by LPC. 24 h after intraventricular LPC injection, we observed elevated expression of the pro-inflammatory cytokines IL-1β and TNFα, and macrophages/microglia were more elongated/activated and localized to the

ventricular wall. Seven days later (at P15), inflammation persisted as evidenced by numerous activated macrophages/microglia within and extruding out of the choroid plexus. In periventricular regions, reactive astrocytes were profusely distributed in white-matter tracts and the levels of chemokines involved in the migration of inflammatory cells were elevated in the cerebrospinal fluid (CSF).

- The immunomodulators minocycline and dexamethasone, each administered daily for 1 week after LPC injection, did not reverse the effects of LPC-induced PHH at P15.
- Combination therapy, using the ATX inhibitor GWJ-23 in conjunction with daily minocycline treatment, failed to rescue the LPC-induced PHH at P15.

Introduction

Intraventricular hemorrhage in neonates is closely associated with the development of post-hemorrhagic hydrocephalus (PHH), a condition resulting in the accumulation of cerebrospinal fluid (CSF) in the neonatal brain that causes increased intracranial pressure, ventriculomegaly (VM), and tissue loss. The hemorrhagic events that produce PHH expose the developing brain to blood components, including LPC, which is converted by autotaxin into its more active form, LPA. The only effective PHH treatment available today is neurosurgical placement and continual life-long replacement of shunts that drain excess CSF and thereby relieve intracranial pressure. However, high infection rates are associated with this treatment, and patients still develop significant long-term cognitive and behavioral deficits.

We previously established a mouse model in which intraventricular injection of LPA into neonatal mice produces effects like human PHH, including increased intracranial pressure (ICP) and ventriculomegaly (Lummis et al. 2019: *$LPA_{1/3}$ overactivation induces neonatal post-hemorrhagic hydrocephalus through ependymal loss and ciliary dysfunction*, Science Advances 5 (10)). This model is an improvement over previous prenatal models because it more closely approximates the stages in human development when PHH typically occurs. In the mouse, LPA acts through one or more of 6 identified receptors ($LPAR_{1\text{-}6}$), and we have used *Lpar1*-deficient mice to determine that LPA's induction of hydrocephalus occurs through an LPAR-dependent mechanism.

Because high levels of LPC are found in human hemorrhagic brains, we adapted this mouse PHH model to focus on LPC's ATX-dependent production of LPA and its downstream consequences. Specifically, we demonstrated that ATX inhibitors (ATXis) can prevent certain elements of LPC-induced hydrocephalus. We also assessed the efficacy of other therapeutic or preventive agents in combating the cellular and molecular changes caused by LPC. In addition, we identified the inflammatory cell types that are recruited to the cerebral ventricles following LPC injection and tested whether anti-inflammatory agents could ameliorate hydrocephalus in this model. Finally, we performed behavioral testing to see if ATX inhibition can improve the cognitive deficits observed in adult mice after neonatal treatment with LPC. Our major accomplishments and challenges are addressed in this final report.

2. KEYWORDS

Autotaxin (ATX)
Autotaxin inhibitor (ATXi)
Cerebrospinal fluid (CSF)
Intracranial pressure (ICP)
Lysophospholipid
Lysophosphatidic acid (LPA)
Lysophosphatidyl choline (LPC)
Lysophosphatidic acid receptor 1 (LPAR1)
Neuroinflammation
Post-hemorrhagic hydrocephalus (PHH)
SWITCH
Ventriculomegaly (VM)

3. ACCOMPLISHMENTS

Major Goals of the Project

The goal of this project was to identify potential new therapies for the prevention and treatment of human hydrocephalus.

Aim 1: Assess the therapeutic effects of blocking ATX-mediated LPA production in PHH models. The overall goal of Aim 1 was to evaluate pharmacological inhibitors of ATX for their ability to prevent LPC-induced PHH in our mouse model. We previously reported that the ATX

inhibitors GLPG 1690 and PF-8380, which are only soluble in DMSO, were not compatible with our system; thus, we used a water-soluble ATXi, GWJ-23.

Aim 2: Assess the interruption of the neuroinflammation associated with PHH. The purpose of this Aim was to determine which neuroinflammatory cell types are recruited to the ependymal surface in response to LPC exposure and which pro-inflammatory cytokines are responsible for their recruitment.

Aim 1 Results

Optimization and baseline effects of LPC injection (Figures 1-4). The LPC model of PHH was characterized in initial studies, which allowed baseline comparisons for both Aims. Assessed parameters included the development of hydrocephalus, and effects on the brain, both grossly and microscopically. In our mouse model of hydrocephalus, we injected vehicle (0.01% fatty acid-free BSA in PBS), as a control, or LPC (in vehicle) into the lateral ventricles of postnatal day 8 (P8) mice, the age that correlates with the 3rd trimester of human pregnancy. Injection of 2.5 mM LPC resulted in visible dome-shaped, macrocephalic heads, and quantifiable ventriculomegaly (VM) typified by ventricular dilation, cortical thinning, and white matter damage (**Figure 1**).

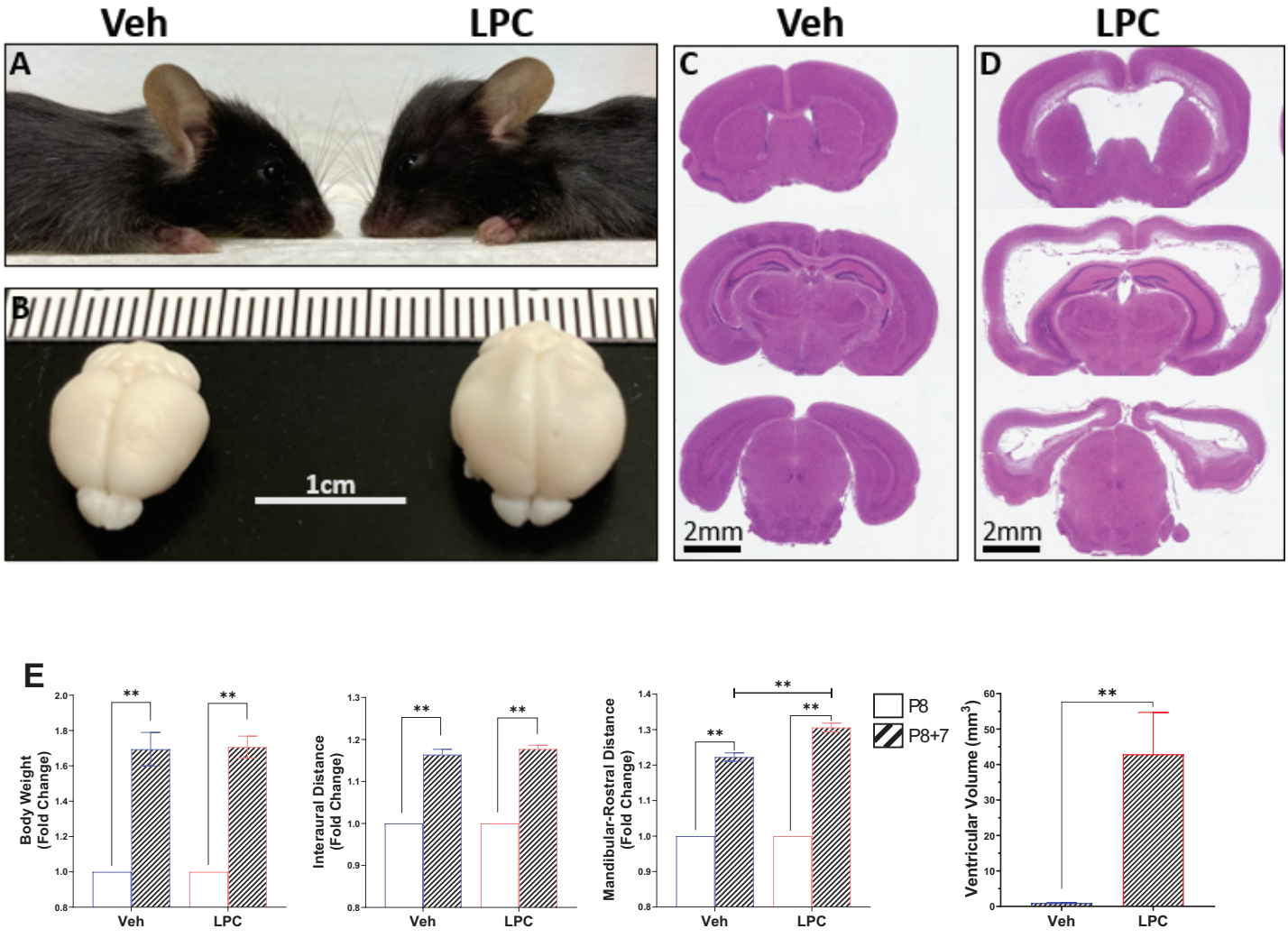

Figure 1. LPC induces hydrocephalus in neonatal mice. Representative images of vehicle-injected and hydrocephalic LPC-injected mice (**A**) and brains (**B**) at P15, 7 days post-injection. (**C** and **D**) H&E-stained coronal brain sections at P15. (**E**) Mice showed normal gains in body weight and interaural (IA) distance regardless of injectant; however, the mandibular-rostral (MR) distance and ventricular volume were significantly increased in LPC-injected subjects. Data are presented as mean ± SEM and were analyzed by 1-way ANOVA using Tukey's post-hoc test (MR distance) or unpaired t-test (VV). ** P<0.01.

Additional histological assessments of intraventricular vehicle or LPC exposure in P15 brains were performed by conventional immunofluorescence staining of fixed, paraffin-embedded brain sections (**Figure 2**) and by sequential immunostaining of perfusion-fixed whole brains via SWITCH (service provided by LifeCanvas Technologies; **Figures 3** and **4**). Both staining techniques independently demonstrated corroborative histopathologic changes that are consistent with PHH development.

Conventional immunolabeling with antibodies against S100A/B (to visualize ependymal cells) and acetylated tubulin (to detect cilia) demonstrated that the vehicle-injected lateral ventricle is lined by a layer of ciliated ependymal cells which form a tight epithelial boundary separating CSF from brain tissue (**Figure 2A**). Exposure to LPC results in a marked loss of the ependymal lining and accompanying denudation of cilia at the ventricular surface (**Figure 2B**). In the corpus callosum, myelin content (as assessed by myelin basic protein, MBP) was seen to be diminished by LPC, while glial fibrillary acidic-protein (GFAP)-immunoreactivity (depicting reactive astrocytes) was augmented (**Figure 2C** and **D**). Along with loss of the ependymal layer, LPC caused a significant reduction of N-Cadherin-based adherens junctions and elicited dense neural progenitor cell/nestin signals at the ventricular surface (**Figure 2E** and **F**). Similarly, LPC induced strong postmitotic neuronal signals (visualized by β-III-tubulin antibody) at the ventricular surface whereas aberrant localization of mitotic cells (by phospho-histone H3 labeling) in the subventricular zone was not as clearly detected (**Figure 2G** and **H**).

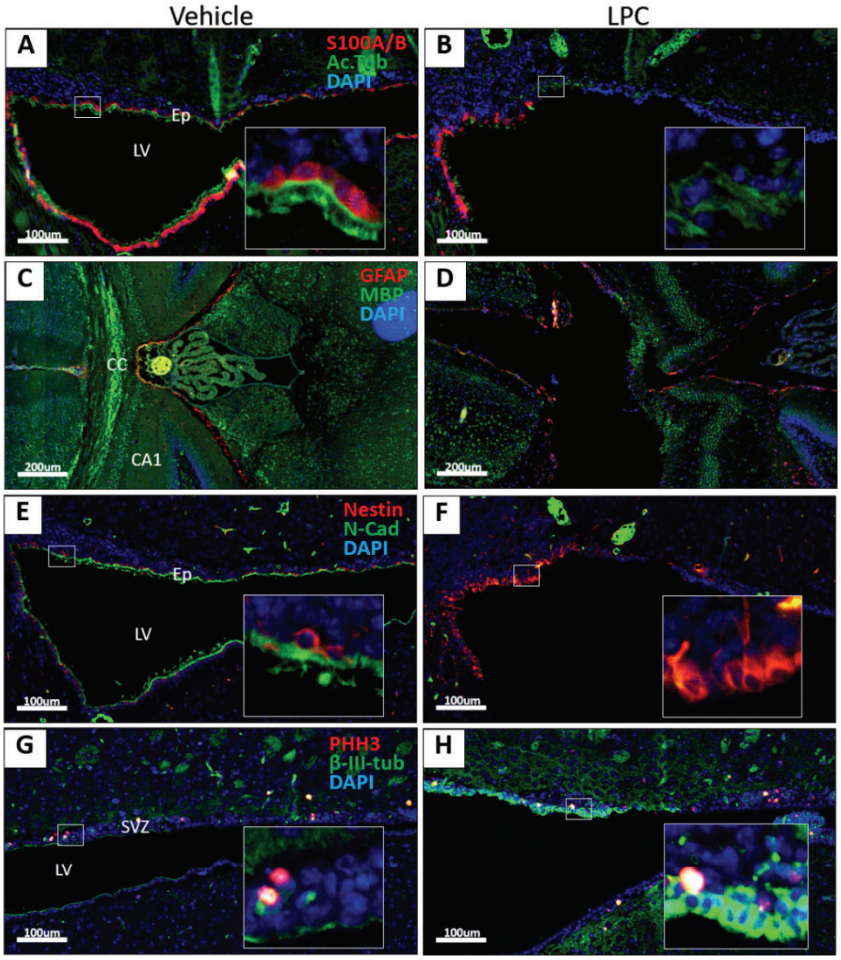

Figure 2. LPC induces histopathologic changes in the neonatal brain. Vehicle or LPC were injected into neonatal mice at P8, and brains were harvested at P15 for histologic assessment. Insets within figures show magnified view of boxed regions. (**A** and **B**) Exposure to LPC, but not vehicle, caused extensive disruption of S100+ ependymal cells (S100A/B, *red*) and resultant loss of cilia (Ac.Tub, *green*) at the lateral ventricle (*LV*)/ependymal (*Ep*) lining. (**C** and **D**) LPC also decreased myelin content (MBP, *green*) and induced astrogliosis (GFAP, *red*) in the corpus callosum (CC). (**E** and **F**) Continuous N-Cadherin (*green*) staining at the ependymal (Ep) surface is abrogated by LPC and replaced by dense nestin (*red*) signals. (**G** and **H**) Whereas the mitotic neural progenitor cell distribution, as assessed by immunolabeling of phosphorylated histone H3 (PHH3, *red*), did not appear to be remarkably altered, there was a significant induction of postmitotic neuronal signal (β-III-tub, *green*) at the SVZ. Antibodies used: anti-S100A/B (Novus Biologicals), anti-Acetylated Tubulin (Sigma-Aldrich), anti-GFAP (Neuromics), anti-MBP (Abcam), anti-Nestin (Abcam), anti-N-Cadherin (BD), anti-PHH3 (Millipore Sigma), and anti-β-III-tubulin (BioLegend). Nuclei were counterstained with DAPI (*blue*).

SWITCH is an antigen-preserving lipid-clearing technique that allows for sequential staining of cellular markers present in specific cell types, in particular brain regions that have been cleared of lipid. This type of analysis is technically challenging as it involves validation of selected antibodies on cleared tissue, data acquisition using a light-sheet microscope, and conversion of the data into a useable format. We stained and imaged two sets of neonatal brains injected with either vehicle or LPC. One set was labeled with antibodies against S100β, GFAP,

and Lycopersicon (to visualize ependymal cells, astrocytes, and vasculature, respectively); the second set was labeled with antibodies specific for MBP, β3-tubulin, and phospho-histone H3 (to visualize myelin, postmitotic neurons, and mitotic cells). No obvious differences in the brain vasculature were observed between P15 brains that had been injected with either vehicle or LPC (**Figure 3A**, **B**, **E**, and **F**). An increase in GFAP-reactive astrocytes was observed in the brain of an LPC-injected mouse near an enlarged cerebral ventricle (**Figure 3C**, **D**, **G**, and **H**).

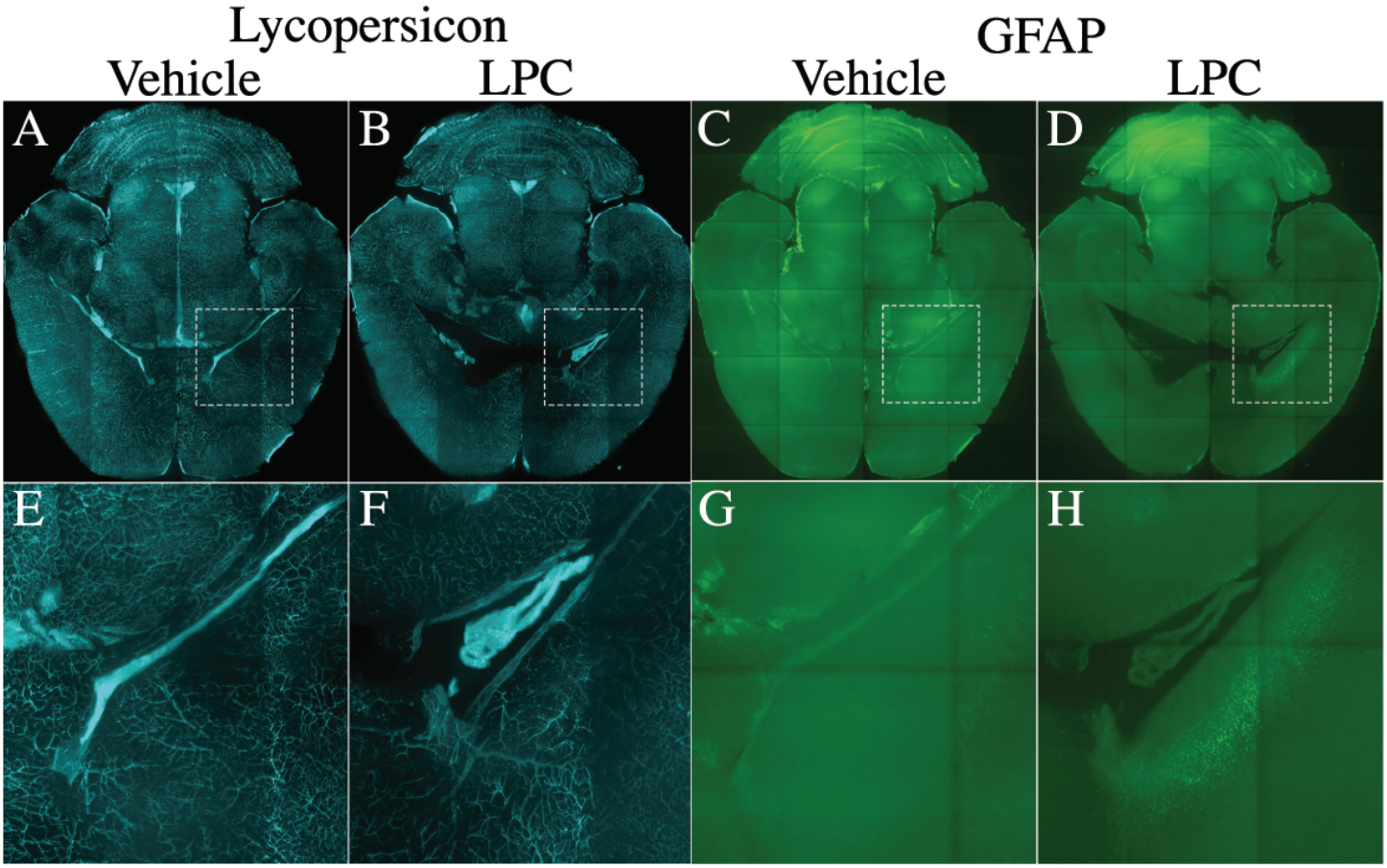

Figure 3. Lycopersicon and GFAP labeling of vehicle- and LPC-injected whole mouse brains using SWITCH. Brains from P15 neonatal mice that were injected intraventricularly with either vehicle or LPC at P8 were excised and processed by SWITCH. (**A-D**) whole brains from vehicle- (**A** and **C**) or LPC-injected mice (**B** and **D**) stained with lycopersicon (from Vector Laboratories, in **A** and **B**) to label blood vessels, or immunolabeled with the fluorochrome-conjugated antibody GFAP (from BioLegend, in **C** and **D**) to detect astrocytes. Areas of **A-D** corresponding to cerebral ventricles are boxed, and shown at higher magnification in **E-G**. A light-sheet microscope was used to serially image through the entire labeled brain. Representative images were acquired from 50 images and processed with Fiji imaging software.

Following SWITCH clearing, myelination (as assessed by MBP immunolabeling) was reduced in whole brains after LPC exposure, compared to vehicle-injected controls (**Figure 4A**, **B**, **E**, and **F**). The induction of GFAP signal and decreased MBP labeling in the cleared, whole brain, are consistent with the findings illustrated in **Figure 2**. Using SWITCH, LPC exposure clearly induced neural progenitor cell mitotic displacement (**Figure 4C**, **D**, **G**, and **H**). These results are consistent with the neural progenitor cell mitotic displacement observed in the embryonic mouse brain following intraventricular injection of LPA (Yung et.al. 2011: *Lysophosphatidic acid signaling may initiate fetal hydrocephalus*, Science Translational Medicine 3(99).

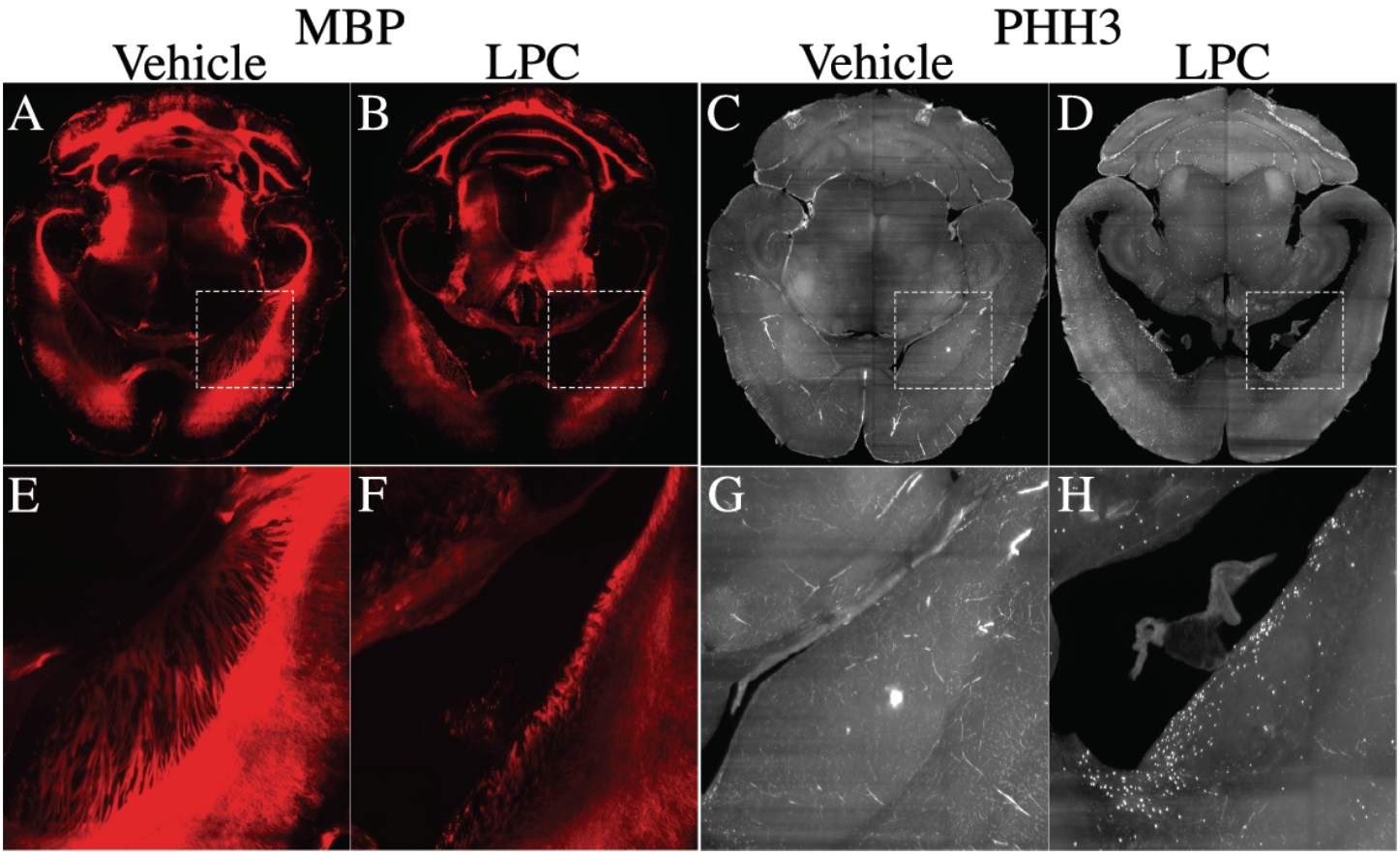

Figure 4. **Myelin basic protein (MBP) and phospho-histone H3 (PHH3) immunolabeling of vehicle- and LPC-injected whole mouse brains using SWITCH**. Brains from P15 neonatal mice that were injected intraventricularly with either vehicle or LPC at P8 were excised and processed by SWITCH. (**A**, **B**, **C**, and **D**) are representative 50 serial image stacks processed with Fiji imaging software of vehicle- (**A** and **C**) and LPC- (**B** and **D**) injected neonatal mouse brains. (**A** and **B**): immunolabeling with an anti-MBP antibody (EnCor Biotechnology) followed by a fluorochrome-conjugated secondary antibody. (**C** and **D**) immunolabeling with a fluorochrome-conjugated anti-phospho-Histone H3 antibody (Millipore Sigma). Areas of **A-D** corresponding to cerebral ventricles are boxed, and shown at higher magnification in **E-H**. A light-sheet microscope was used to acquire serial images through the labeled brains.

Effects of GWJ-23 on LPC-induced hydrocephalus. To determine if the ATXi, GWJ-23, can prevent LPC-induced hydrocephalus, P8 mice were pre-injected with either 2.5 µl of vehicle, or one of two different concentrations of GWJ-23: 26 µM or 130 µM; the animals were then re-injected 15 minutes later with 2.5 µl of either vehicle or 5 mM LPC. Body weight and head-size measurements were recorded at P8 prior to injection, and 1 week later at P15 (**Figure 5A**). Brains from all injected animals were fixed, embedded, sectioned, and stained to assess ventricular size, ependymal integrity, myelin content, and macrophage infiltration (**Figure 5B**). Whereas our initial data indicated that pre-injection with 26 µM GWJ-23 reduced the severity of LPC-induced VM relative to controls, our final data demonstrated that there is no statistically significant prevention of gross or histological hydrocephalus by either 26 µM or 130 µM GWJ-23, at 1-week post-injection.

Aim 1.2: Assess surrogate endpoints for quality-of-life following PHH preventative treatment using mouse behavioral tests.

We previously conducted behavioral tests on cohorts of mice that were injected with either vehicle or LPC at P8, and observed significant gait abnormalities, and some deficits in grip strength, motor coordination, and exploratory behavior, as presented in past Progress Reports.

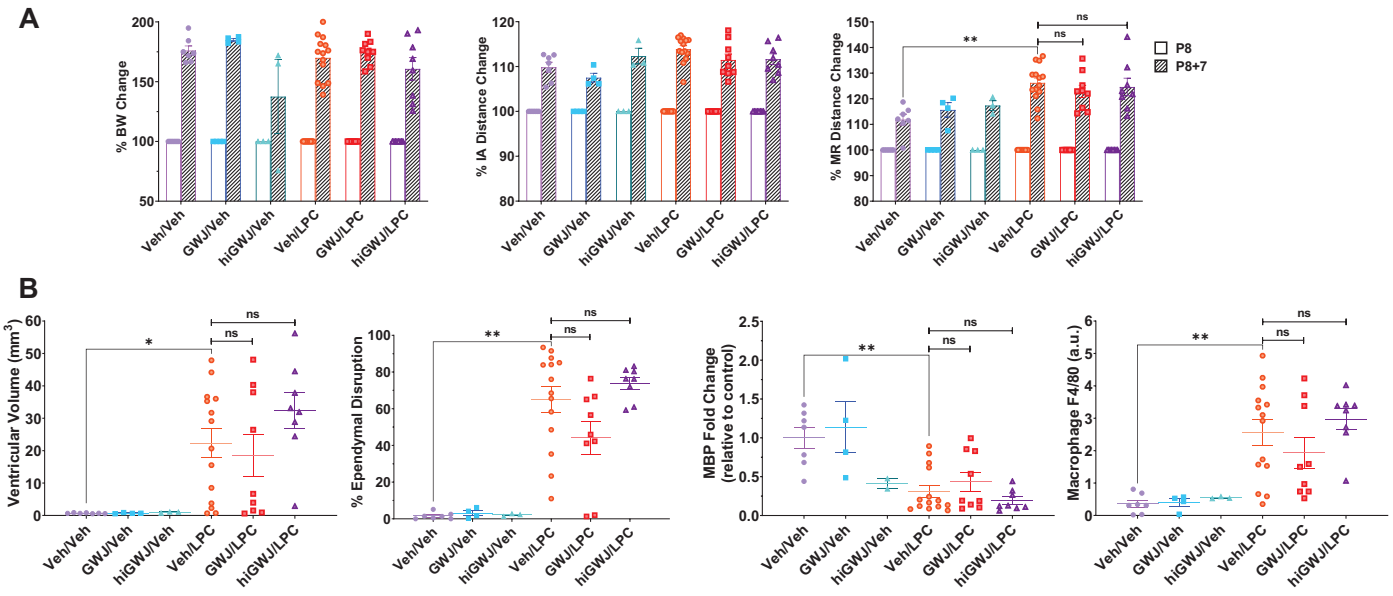

Figure 5. The ATXi GWJ-23 does not prevent LPC-induced hydrocephalus. (**A**) Body weight (*BW*) and head size (*IA-* or *MR Distance*) were measured at P8 (day of injection) and P15 (day of sacrifice). *GWJ:* 26 µM GWJ-23; *hiGWJ:* 130 µM GWJ-23; *Veh*: vehicle. (**B**) Coronal sections of brains at P15 were stained and analyzed. Ventricular volume was calculated by measuring the area of the lateral ventricles in serial, H&E-stained coronal sections spaced at 200 µm intervals. Ependymal integrity was determined from H&E-stained sections. Myelin integrity was assessed by MBP staining and macrophage density was ascertained using Leica Aperio ImageScope software to calculate: (i) MBP fluorescence intensity in the corpus callosum, or (ii) F4/80-DAB intensity in the periventricular region. Each *dot* represents one brain analyzed. Data are presented as mean ± SEM and were analyzed by 1-way ANOVA using Tukey's post-hoc test. * P<0.05; ** P<0.01; *ns*, not significant.

To examine whether ATX inhibition could rescue the LPC-induced behavioral deficits, four cohorts of mice were pre-injected with 2.5 µl of vehicle or 26 µM GWJ-23, followed by 2.5 µl of vehicle or 5 mM LPC, 15 minutes later. A total of 24 mice were injected, and behavioral tests were performed at the following ages: gait analysis at P52-54, open-field at P56-57, hanging-wire and Y-maze at P58-59, novel-object recognition at P62-64, and Barnes maze at P69-86. As advised by Dr. Amanda Roberts, Director of the Mouse Behavioral Assessment Core at Scripps Research, the common acceptable minimum age for behavioral testing is 8-10 weeks.

Unfortunately, and unexpectedly, LPC drastically compromised the survival of the Veh/LPC and GWJ/LPC cohorts (**Figure 6**). This was likely due to a batch effect of LPC, with the fresh compound eliciting a much more severe phenotype. Nevertheless, gait analysis, hanging-wire, Y-maze, and open-field tests were performed as planned, and the results are presented in **Table 1**. Due to the high mortality of LPC cohorts, the cognitive and memory tests (novel-object recognition and Barnes maze) could not be analyzed. The mice from the Veh/LPC cohort that died were severely hydrocephalic, as were the ones from the GWJ/LPC cohort. Interestingly, whereas 8 of 9 Veh/LPC mice did not survive past 8 weeks of age, 5 of 10 GWJ/LPC mice did, suggesting that GWJ-23 may show some protective effects against LPC. The data presented are therefore *not* an accurate representation of the LPC cohorts since the temporal design of the experiment preferentially selects for subjects with much milder manifestations of the disease. However, taken together with results presented in previous Progress Reports, we surmise that LPC-induced PHH is associated with changes in gait (particularly stride length), and deficits in grip strength, motor coordination, ambulation, and exploratory behavior, and that GWJ-23 appears to partially restore these outcomes (compare gait analysis, hanging-wire test, and open-field test results of GWJ/LPC cohort to Veh/LPC and Veh/Veh cohorts, **Table 1**).

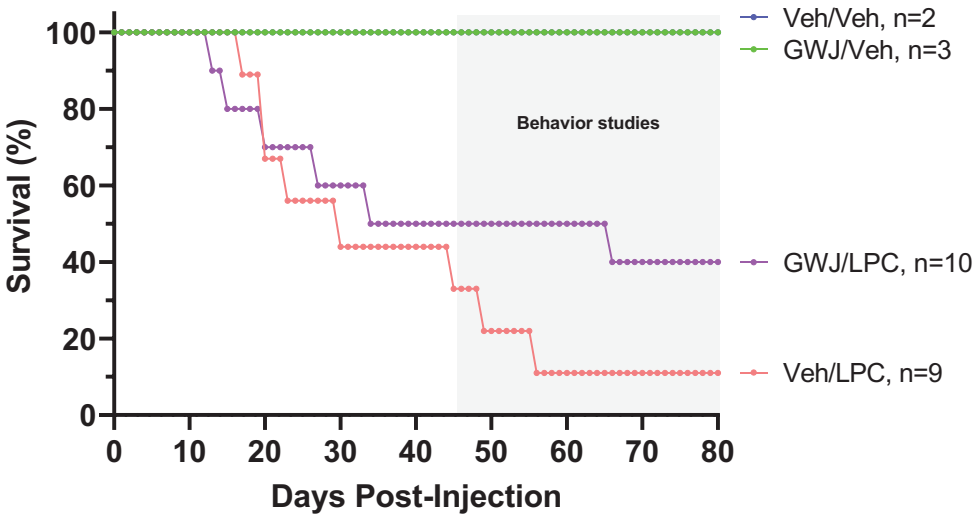

Figure 6. Survival curve of mice that were injected at P8 to perform behavioral studies. Four cohorts were injected, as illustrated, and behavioral analyses were conducted during the indicated period (*grey*).

BEHAVIOR TEST	MOUSE COHORT			
	Veh/Veh	GWJ/Veh	Veh/LPC	GWJ/LPC
GAIT ANALYSIS				
(a) Stride Length (cm):				
-Front	6.20 ± 0.42 (2)	5.70 ± 0.30 (3)	4.57 ± 1.12 (3)	5.68 ± 0.85 (5)
-Hind	6.15 ± 0.50 (2)	5.68 ± 0.11 (3)	4.40 ± 1.19 (3)	5.54 ± 0.88 (5)
(b) Stride Width (cm):				
-Front	1.44 ± 0.05 (2)	1.54 ± 0.09 (3)	1.64 ± 0.11 (3)	1.55 ± 0.25 (5)
-Hind	2.42 ± 0.33 (2)	2.24 ± 0.41 (3)	2.21 ± 0.33 (3)	2.32 ± 0.36 (5)
HANGING WIRE				
(a) Score (0-5)	4.00 ± 0.95 (2)	4.00 ± 1.20 (3)	2.84 ± 3.07 (2)	3.33 ± 2.10 (5)
(b) Time (secs)	30.00 ± 0.00 (2)	26.89 ± 5.39 (3)	16.00 ± 19.80 (2)	20.27 ± 12.96 (5)
Y-MAZE				
(a) Total Entries	32.50 ± 2.12 (2)	41.33 ± 1.16 (3)	23.00 ± 25.46 (2)	29.20 ± 14.20 (5)
(b) % Spontaneous Alternations	63.53 ± 11.82 (2)	54.34 ± 5.50 (3)	58.98 ± 10.88 (2)	67.76 ± 18.80 (5)
OPEN FIELD				
(a) Total Distance Traveled (cm)	22678 ± 4507 (2)	23034 ± 6951 (3)	13246 ± 10747 (2)	21543 ± 6584 (5)
(b) % Time in Center	39.52 ± 1.49 (2)	28.69 ± 17.70 (3)	22.92 ± 23.71 (2)	33.59 ± 4.43 (5)

Table 1. Behavioral measurements for gait, hanging-wire, Y-maze, and open-field tests. Data are presented as mean ± SD (n).

AIM 1 PRIMARY FINDINGS

- Injection of 2.5 mM LPC into the lateral ventricles of P8 mice results in the development of hydrocephalus characterized by VM, ependymal cell loss, myelin loss, and microglia/macrophage infiltration.
- Conventional immunofluorescence staining of brain sections and SWITCH staining of whole, cleared brains demonstrated a similar histopathology caused by LPC exposure including (i) myelin loss, (ii) increased GFAP-reactive astrocytes, and (iii) neural progenitor cell mitotic displacement.
- Blocking ATX-mediated LPA production using GWJ-23 did not prevent LPC-induced PHH assessed at P15 (1 week after LPC exposure) but may protect against LPC-associated mortality.
- While not statistically significant, LPC-induced changes in gait (particularly stride length), and deficits in grip strength, motor coordination, ambulation, and exploratory behavior appeared to be partially restored by GWJ-23.

Aim 2 Results

Aim 2.1: Examine the neuroinflammatory sequelae following induction of hydrocephalus.

In humans, ventricular shunts are frequently obstructed by immune cell infiltration which necessitates continual replacement over a patient's lifetime. The affected inflammatory cells include macrophages, microglia, and reactive astrocytes that are present in the ventricular lining of fetal hydrocephalic brains. In neonatal mice, LPA exposure leads to an influx of phagocytic cells on the ciliated ependymal cell surface, as well as significant increases in neutrophil and microglia or resident/infiltrating macrophages detected in whole brains. However, the types of inflammatory cells involved in LPC-induced PHH, and their roles in hydrocephalus development, are not well understood. The purpose of this Aim was to determine which inflammatory cell types are recruited to the ependymal surface in response to LPC exposure and which pro-inflammatory cytokines are responsible for their recruitment.

In our previous update we showed that 24 hours following injection at P8, there was a significant induction of expression of the pro-inflammatory cytokines IL-1β and TNFα in the LPC-exposed brains. Immunofluorescence staining for ionized calcium-binding adaptor molecule 1 (Iba1) 24 hours after injection showed that Iba1, which is specifically upregulated during activation of microglia and macrophages, was present in the choroid plexus and periventricular regions of brains exposed to either vehicle or LPC. In the lateral ventricles of LPC-injected brains, we observed an increased number of elongated Iba1+ cells (suggestive of activated microglia) that appeared to have extravasated out of the choroid plexus to the ependymal surface of the ventricle.

To determine whether these LPC-induced neuroinflammatory effects persist past 24 hours, we examined P15 brains harvested 7 days following vehicle or LPC exposure. There was an increased number of macrophages detected in the LPC-injected brain using the macrophage-specific F4/80 clone Cl:A3-1 antibody, which also stains microglia (macrophages of the central nervous system; **Figure 7**), particularly in the choroid plexus of the dilated

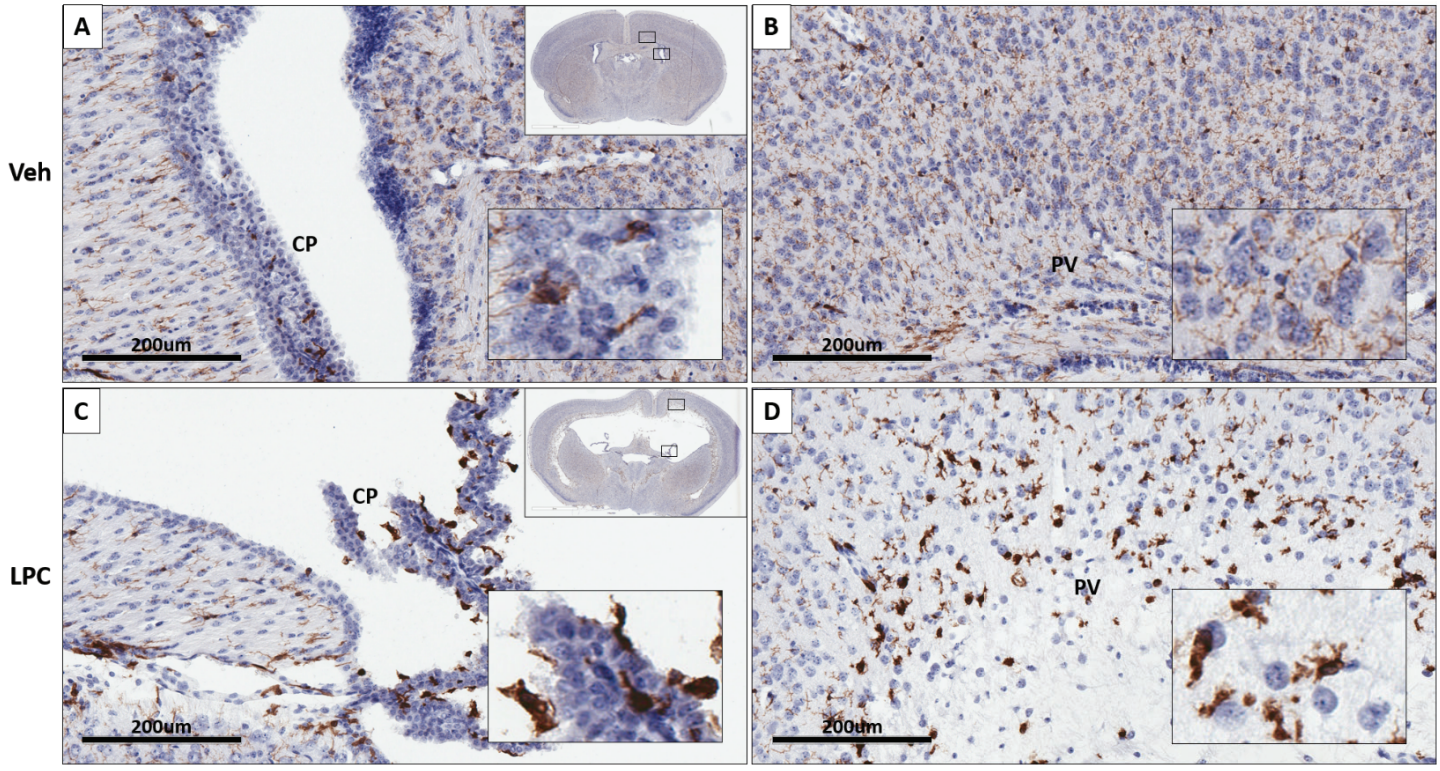

Figure 7. LPC induced an increase in macrophages/microglia in the choroid plexus and periventricular region. Mice were injected at P8 with vehicle (**A** and **B**) or 2.5 mM LPC (**C** and **D**), then the brains were harvested at P15, fixed, processed, and paraffin-embedded. Brains were sectioned coronally and 10 μm sections were stained with an anti-F4/80 antibody (BioRad) and detected by DAB/peroxidase (Vector Laboratories). Representative images of vehicle- and LPC-exposed brain sections depicting basal levels of F4/80-immunoreactive cells in vehicle-injected brains (**A** and **B**) and pronounced increase in macrophage/microglial signal in LPC-injected brains (**C** and **D**). Bottom-right *insets* in **A-D** depict magnified views of the choroid plexus (CP) in **A** and **C**, and of the periventricular (PV) regions in **B** and **D**.

ventricle. Additionally, whereas these F4/80+ cells were situated within the choroid plexus of the vehicle-injected brain, many F4/80-immunoreactive cells appeared to have extruded out of the choroid plexus in the LPC-injected brain. Notably, the morphologies of the F4/80+ cells were very different in the LPC- vs. vehicle-exposed brains: whereas the cells in the vehicle-injected brain had small somas and ramified processes typical of resting-state (homeostatic) microglia, the cells in the LPC-injected brain had large somas and retracted processes, representative of activated microglia.

Concomitant with this increase in the number of macrophage/microglial cells 7 days post-injection, significant astrogliosis was also observed in LPC-exposed brains. Immunohistochemical staining for GFAP, which is highly expressed in reactive astrocytes, showed an abundance of GFAP+ cells in the LPC-injected brains, particularly in the corpus callosum and white matter tracts (**Figure 8**).

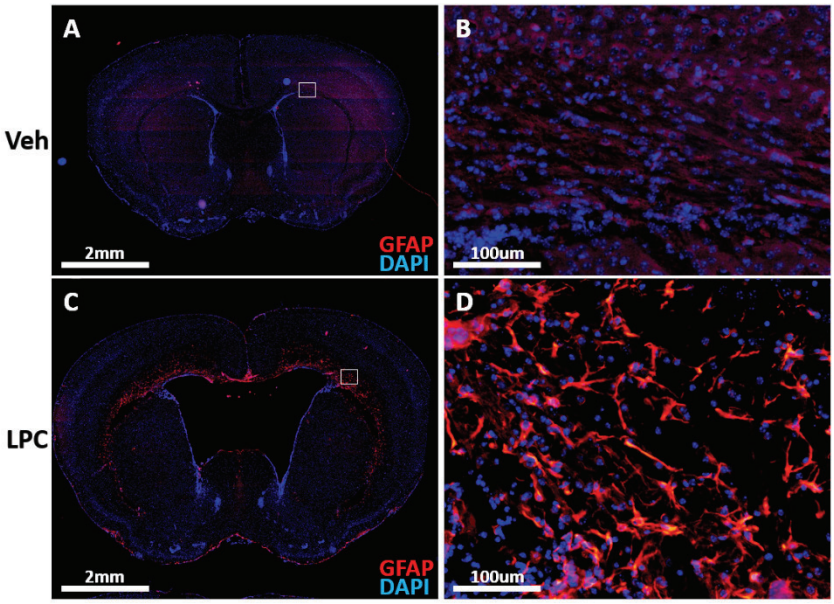

Figure 8. LPC-induced astrogliosis in the corpus callosum and white matter tracts. Mice were injected with vehicle (*top panels*) or 2.5 mM LPC (*bottom panels*) at P8, then brains were harvested at P15, fixed, processed, and embedded in paraffin. Brains were sectioned coronally and 10 µm sections were immunostained with a GFAP antibody (Neuromics) to visualize astrocytes (*red*) and nuclei were counterstained with DAPI (*blue*). **A** and **B**: Representative images of vehicle-injected brain sections depicting low levels of GFAP signal. **C** and **D**: Representative images of LPC-injected brain sections indicating high levels of GFAP immunoreactivity in the white matter. Boxed areas in **A** and **C** are magnified and shown in **B** and **D,** respectively.

Analysis of inflammatory cytokines in hydrocephalic CSF. CSF was extracted from LPC-injected hydrocephalic brains at P15 and analyzed using a mouse cytokine multiplex panel (service provided by IDEXX BioAnalytics). As expected, there was some degree of variability between individual samples, but there were several distinct differences in the hydrocephalic CSF from LPC-injected brains vs. the CSF from controls. A summary of the data is provided in **Table 2**. The cytokines/chemokines which appeared to show consistent downward or upward trends in CSF derived from LPC-injected brains, as compared to controls, are indicated in *blue* and *red,* respectively. The levels of pro-inflammatory cytokines IL-1β and TNFα were not different between control and LPC CSF samples. This result agrees with our qPCR data from whole brain homogenates whereby expression of these cytokines was induced at 24 hours after LPC insult but returned to baseline and/or were equivalent to those of the vehicle-injected brains at P15 (presented in a prior update). Overall, cytokine levels were either similar or decreased in the LPC CSF samples when compared to controls. However, the levels of several chemokines were augmented in the LPC CSF samples. Specifically, levels of the chemokines CXCL10/IP-10 and CCL4/MIP-1β (chemoattractants for CD4+ T cells), CXCL1/MKC (a chemoattractant for neutrophils), and CCL2/MCP-1 (a chemoattractant for monocytes), were all found to be elevated in the CSF from LPC-injected brains. These findings implicate an influx of a myriad immune cells into the LPC-injected lateral ventricle and supports our inflammation-related immunohistochemical data.

SAMPLE	1 Control CSF	2 LPC CSF	3 LPC CSF	4 LPC CSF	5 LPC CSF	6 LPC CSF	7 LPC CSF
IL-1α (pg/mL)	603.3	149.6	103.4	84.7	68.9	192.42	251.6
IL-1β (pg/mL)	<16	<16	<16	<16	<16	<16	<16
IL-2 (pg/mL)	18.3	21.9	<3.2	16.0	<3.2	17.5	47.7
IL-4 (pg/mL)	<3.2	<3.2	<3.2	<3.2	<3.2	<3.2	<3.2
IL-5 (pg/mL)	<3.2	<3.2	<3.2	<3.2	<3.2	<3.2	<3.2
IL-6 (pg/mL)	19.68	<3.2	<3.2	<3.2	<3.2	<3.2	<3.2
IL-7 (pg/mL)	<16	<16	<16	<16	<16	<16	<16
IL-9 (pg/mL)	997.2	629.2	570.5	439.0	431.9	987.9	1272.1
IL-10 (pg/mL)	65.0	23.6	45.2	17.1	36.9	40.1	41.4
IL-12(p40) (pg/mL)	192.54	54.05	77.4	63.74	70.54	85.08	156.7
IL-12(p70) (pg/mL)	<16	<16	<16	16.1	<16	<16	<16
IL-13 (pg/mL)	190.9	64.5	120.7	68.6	<64	143.4	258.4
IL-15 (pg/mL)	195.4	<80	<80	<80	<80	<80	<80
IL-17 (pg/mL)	<3.2	6.3	<3.2	5.3	<3.2	<3.2	9.1
G-CSF (pg/mL)	<3.2	<3.2	<3.2	<3.2	<3.2	<3.2	<3.2
GM-CSF (pg/mL)	<16	48.3	<16	<16	<16	<16	<16
INFγ (pg/mL)	<3.2	<3.2	<3.2	<3.2	<3.2	<3.2	<3.2
CXCL10/IP-10 (pg/mL)	38.58	95.19	219.82	135.58	276.38	206.18	179.02
CCL1/MKC (pg/mL)	64.64	115.5	160.1	147.9	189.58	138.50	161.40
CCL2/MCP-1 (pg/mL)	33.9	70.3	39.5	52.4	42.2	49.82	76.08
CCL3/MIP-1α (pg/mL)	224.9	143.0	<80	157.6	<80	195.7	345.5
CCL4/MIP-1β (pg/mL)	<80	148.0	163.9	137.6	181.6	165.1	180.08
CXCL2/MIP-2 (pg/mL)	<80	<80	<80	<80	<80	<80	<80
CCL5/RANTES (pg/mL)	57.2	38.9	36.0	37.3	<16	51.1	88.36
TNFα (pg/mL)	<16	18.6	<16	<16	<16	<16	<16

Table 2. Mouse cytokine panel results. CSF was extracted from P15 mice that were injected with LPC on P8. Each LPC CSF sample was derived from an individual mouse. Control CSF was pooled from 5 mice from the same genetic background since the volume of CSF that can be obtained from an individual, non-hydrocephalic mouse brain is very small. Analytes that were decreased in LPC-affected CSF, as compared to control CSF, are denoted in *blue*; analytes that were increased in LPC CSF are denoted in *red*.

Aim 2.2: Assess hydrocephalic phenotypes following combination therapy of LPA signaling inhibition and immunomodulators.

The purpose of this Aim was to test whether immunomodulators could suppress the neuropathological effects of PHH. As reported in our previous update, neither minocycline (45 mg/kg) nor dexamethasone (0.5 mg/kg), administered intraperitoneally immediately following injection, and daily thereafter for 7 days, prevented LPC-induced VM or macrophage infiltration. We now report that, similarly, neither ependymal integrity nor myelin content were restored by treatment with either agent (**Figure 9**).

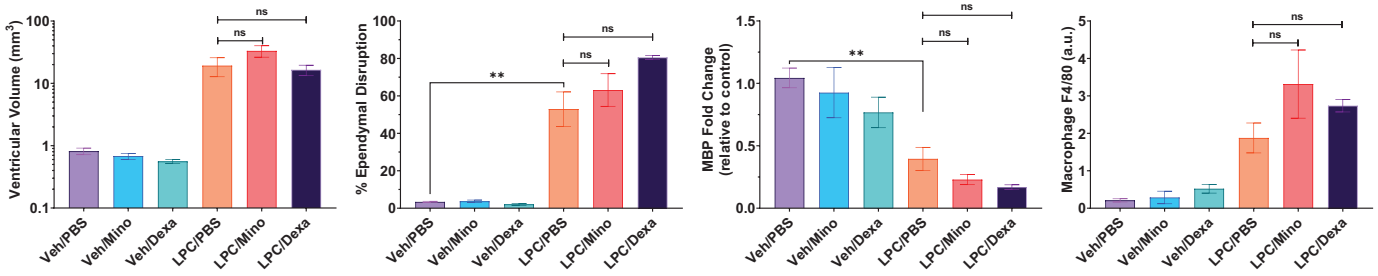

Figure 9. Effects of minocycline and dexamethasone on LPC-induced hydrocephalus. P8 mice were injected with vehicle or 2.5 mM LPC, then the mice immediately received daily intraperitoneal injections of PBS (control), 45 mg/kg minocycline (*Mino*), or 0.5 mg/kg dexamethasone (*Dexa*), until the brains were harvested at P15. Data are presented as mean ± SEM, sample size (n) range of 3-12. ** P<0.01; *ns*, not significant.

Next, we investigated whether minocycline could suppress LPC-induced hydrocephalus in P8 mice if administered in combination with ATX inhibition. To do so, we first stereotactically injected 2.5 µl vehicle or 26 µM GWJ-23, waited 15 minutes, then injected 2.5 µl of vehicle or 5 mM LPC. Immediately afterward, mice were injected intraperitoneally with PBS (control) or minocycline (45 mg/kg), and administered this treatment daily for 7 days, after which the brains were harvested at P15 for analyses. We found that the combination of GWJ-23 and minocycline was still insufficient to reduce LPC's effects on VM, ependymal cell and myelin loss, or macrophage infiltration (**Figure 10**).

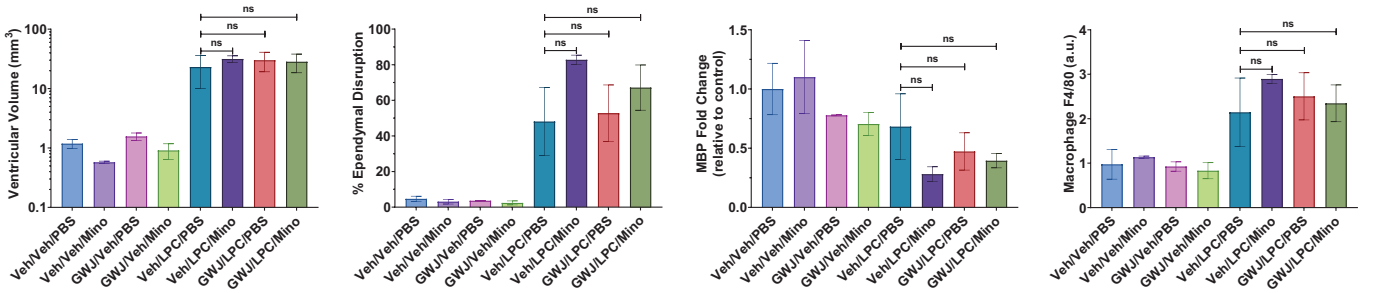

Figure 10. Effects of combined GWJ-23 and minocycline treatments on LPC-induced hydrocephalus. P8 mice were injected with 2.5 µl of vehicle or 26 µM GWJ-23 followed by 2.5 µl of vehicle or 5 mM LPC, then the mice received daily intraperitoneal injections of PBS (control) or 45 mg/kg minocycline (*Mino*) until the brains were harvested at P15. Data are presented as mean ± SEM, sample size (n) range 2-6; *ns*, not significant.

AIM 2 PRIMARY FINDINGS

- At P9, 24 hours following injection of LPC into the lateral ventricle, we observed acute inflammatory responses including (i) induction of IL-1β and TNFα expression, and (ii) activation of macrophage/microglia in the ventricle.
- At P15, 7 days following injection of LPC into the lateral ventricle, we observed further inflammatory responses including (i) increased numbers of activated macrophage/microglia within, and extruding out of, the choroid plexus, as well as in the periventricular regions, (ii) induction of astrogliosis in the white matter tracts, and (iii) increased levels of chemokines that are involved in the migration of inflammatory cells into the ventricle.
- Daily administration over a 1-week period of the immunomodulators minocycline or dexamethasone did not reverse the effects of LPC-induced PHH.
- Combination therapy, via ATX inhibition and daily minocycline treatment, did not prevent or inhibit LPC-induced PHH.

Opportunities for Training and Professional Development

The IDP Statement for Dr. Whitney McDonald is included below.

Dissemination of Results

A manuscript detailing the LPC model and ATX inhibition is in preparation.

Goals for the Next Reporting Period

Nothing to report.

4. IMPACT

The experiments performed in this study will aid the scientific community by increasing our knowledge about how lysophospholipids, particularly LPC, act to produce PHH. We now have a better understanding of 1) the concentrations of injected lysophospholipids required to reliably produce hydrocephalus in our mouse model, 2) the types of immune cells that infiltrate the brain after lysophospholipid exposure, 3) the cytokines that are elevated in response, 4) the effects of LPC on cellular activation, particularly on astrocytes and F4/80-positive cells, and 5) which pharmacological agents should be pursued further. We also developed a better methodology regarding the preparation, storage, and use of lysophospholipids like LPC and LPA, and have further characterized this mouse model of PHH, both of which represent strong contributions to the research community. Overcoming the technical challenges of difficult techniques such as CSF extraction and the analysis of SWITCH images will also improve the cohort of methodologies available to scientists using mice to understand neuropathology. Perhaps most importantly, the characterization of the immune cells that infiltrate the brain following lysophospholipid exposure, and the resultant cytokine production, may represent excellent targets for the development of hydrocephalus therapies or preventive treatments.

Impact on other disciplines

Nothing to report.

Impact on technology transfer

Nothing to report.

Impact of society beyond science and technology

Nothing to report.

5. CHANGES/PROBLEMS

Changes in approach and reasons for change

Several attempts were made to implant human shunt material into mouse brains to identify the cell types that accumulate and block these shunts during hydrocephalus. However, unforeseen technical difficulties, such as the malleability of the shunt material and problems in keeping the shunt in place after insertion into the P8 mouse ventricle, prevented completion of this part of study using the proposed experimental approach.

Two attempts were made to identify and quantify the specific immune cell populations that infiltrate the neonatal brain 24 hours following LPC exposure. Brains were enzymatically and mechanically disaggregated at specified timepoints, and immune cells were isolated by Percoll gradient centrifugation. However, despite many attempts, we could not overcome the technical problems encountered in using the flow cytometer in this paradigm. This prevented us from determining, in detail, the identity, proportion, and number of immune cells in the single cell

suspensions derived from vehicle- and LPC-injected mouse brains. Based on LPC-induced increases in the number of IbaI- and F4/80-positive cells (as shown by immunofluorescence and immunohistochemistry), increases in myeloid cell types would be an expected outcome. It is also possible that other immune cell types, including $CD4^+$ and $CD8^+$ T cells, as well as B cells, infiltrate the neonatal mouse brain following LPC exposure; these cell populations were detected in a previous study in P8 mouse brains, 24 hours after LPA exposure.

Neuroinflammatory modulation on LPC-induced behavioral changes was not attempted. The failure of minocycline and dexamethasone to rescue LPC-induced PHH at P15 gave us no grounds to justify pursuing this experiment.

Actual or anticipated problems or delays and strategies for their resolution

Nothing to report.

Changes that had a significant impact on expenditures

Nothing to report.

Significant changes in use or care of human subjects

Nothing to report.

Significant changes in the use or care of vertebrate animals

Nothing to report.

Significant changes in use of biohazards and/or select agents

Nothing to report.

6. PRODUCTS

Publications, Conference Papers, and Presentations

Journal Publications

McDonald WS, Miyamoto K, Rivera R, Kennedy G, Almeida BSV, Kingsbury MA, Chun J. Altered cleavage plane orientation with increased genomic aneuploidy produced by receptor-mediated lysophosphatidic acid (LPA) signaling in mouse cerebral cortical neural progenitor cells. **Mol Brain** 2020;13(1):169. PMC7734743. Federal support acknowledged.

Puigdomenech-Poch M, Martinez-Muriana A, Andres-Benito P, Ferrer I, Chun J, Lopez-Vales R. Dual role of lysophosphatidic acid receptor 2 (LPA_2) in amyotrophic lateral sclerosis. **Front Cell Neurosci** 2021;15:600872. PMC8026865. Federal support acknowledged.

Ray M, Kihara Y, Bornhop DJ, Chun J. Lysophosphatidic acid (LPA)-antibody (504B3) engagement detected by interferometry identifies off-target binding. **Lipids Health Dis** 2021;20(1):32. PMC8048308. Federal support acknowledged.

Rivera R, Williams NA, Kennedy GG, Sánchez-Pavón P, Chun J. Generation of an *Lpar1* fusion knock-in transgenic mouse line. **Cell Biochem Biophys.** *Accepted pending minor revision, May 2021*. Federal support acknowledged.

Books or Other Non-Periodical, One-time Publications

Nothing to report.

Other Publications, Conferences Papers, and Presentations

Nothing to report.

Website(s) or other Internet site(s)

Nothing to report.

Technologies or Techniques

Nothing to report.

Inventions Patent Applications, and/or Licenses

Nothing to report.

Other Products

Nothing to report.

7. PARTICIPANTS & OTHER COLLABORATING ORGANIZATIONS

Project Participants

Name	Jerold Chun, MD, Ph.D.
Project Role	Principal Investigator
Research Identifier (e.g., ORCID ID)	0000-0003-3964-0921
Nearest person month worked	2.52
Contribution to project	Dr. Chun has primary responsibility for all manuscripts and will determine publication timing and priorities.
Funding support	NIH U01 MH11428, NIH R01 AG065541, NIH R01 AG071465, Janssen R&D SA 21-005, Novartis CSRA 18-09 (completed)

Name	Richard Rivera, Ph.D.
Project Role	Senior Staff Scientist
Research Identifier (e.g., ORCID ID)	0000-0001-6138-3306
Nearest person month worked	1.85
Contribution to project	Dr. Rivera oversees researchers, collects data, and writes and submits animal protocols and amendments to IACUC.
Funding support	N/A

Name	Valerie Tan, Ph.D.
Project Role	Research Specialist
Research Identifier (e.g., ORCID ID)	N/A
Nearest person month worked	3.75
Contribution to project	Dr. Tan performs experiments using the fetal and neonatal mouse models and she will also assess ATX inhibitors.
Funding support	N/A

Name	Laura Wolszon, Ph.D.
Project Role	Scientific Associate
Research Identifier (e.g., ORCID ID)	N/A
Nearest person month worked	3.16
Contribution to project	Dr. Wolszon is responsible for project management activities.
Funding support	N/A

Name	Whitney McDonald, Ph.D.
Project Role	Postdoctoral Associate
Research Identifier (e.g., ORCID ID)	N/A
Nearest person month worked	2.50
Contribution to project	Dr. McDonald was responsible for the embryonic LPC mouse model. She left the lab in January 2020.
Funding support	Dr. McDonald was paid from SBP discretionary funds from 9/1/2019-9/30/2019.

Name	Emily Bornhop
Project Role	Research Assistant I
Research Identifier (e.g., ORCID ID)	N/A
Nearest person month worked	3.00
Contribution to project	Ms. Bornhop genotypes the mice.
Funding support	N/A

Name	Joshua Kurtz
Project Role	Lab Assistant II
Research Identifier (e.g., ORCID ID)	N/A
Nearest person month worked	4.50
Contribution to project	Mr. Kurtz assists with basic experimental setup and lab maintenance.
Funding support	N/A

Changes in PI and Senior/Key Active Other Support

Chun, Jerold

New Active Support from Previously Reported

SA 21-005 (Chun, PI) 10/30/20-10/30/22 1%
Janssen R&D (aka Johnson & Johnson) $266,667 Direct Costs 0.12 calendar
Investigate mode of action of ponesimod in the CNS
Janssen Contact: Anindya Bhattacharya, (858) 320-3424, ABhatta2@its.jnj.com

Completed Support from Since Previously Reported

CSRA 18-09 (Chun, PI) 05/08/18-12/31/20 1%
Novartis Pharma AG $366,878 Direct Costs 0.12 calendar
Siponimod S1P receptor mechanisms in the human CNS
Novartis Contact: Ursula Reichenstein, +4161 696 44 30, ursula.rechenstein@novartis.com

Partnering Organizations

N/A

8. SPECIAL REPORTING REQUIREMENTS

Nothing to report.

9. APPENDICES

N/A

Individual Development Plan

The Sanford Burnham Prebys Medical Discovery Institute (SBP) Office of Education, Training & International Services (OETIS) oversees and coordinates an annual individual development planning (IDP) process for all postdocs at the Institute. The focus of the IDP process at SBP is the career goal of the postdoc; identification of what skills, knowledge, and accomplishments will be necessary for the postdoc to obtain a desired independent position following training; and identification of training and professional development opportunities that are available for the postdoc to obtain the necessary skills and knowledge. The SBP Office of Education, Training & International Services provides guidance and advising to both postdocs and PIs throughout the postdoc's training with respect to developing IDPs and preparing for a successful transition to independence post-training. The SBP Office of Education, Training & International Services also maintains webpages containing comprehensive resources on career path identification, career planning, and creating an IDP that can be utilized in conjunction with the formal annual IDP process.

The SBP IDP process includes two components:

1) **First-Year IDP (effective in 2014).** Within the first 3 months of beginning postdoctoral training at SBP, all postdocs receive and fill out an initial "planning and expectations" document to discuss with their PI. This document serves as the foundation for their postdoctoral IDP and is designed to facilitate discussion between the PI and new postdoc regarding goals and expectations for the first year of training, as well as stimulate initial discussions about long-term career goals and training plans.

2) **Postdoctoral IDP (effective January 2013).** At the end of the first year of training SBP postdocs receive notification that it is time to update their IDP, and they receive the information they included in their first-year planning and expectations document in the form of a full IDP that they can update with their accomplishments over the past year and their goals for the coming year, mid-term future, and long-term future. Each subsequent year of their postdoctoral training, postdocs will receive notification and the previous year's IDP form to update and expand. The IDP forms are designed to build upon each previous year as well as provide a solid foundation from which a postdoc can easily build his or her CV/resume.

The SBP Office of Education, Training & International Services also maintains webpages containing comprehensive resources on career path identification, career planning, and creating an IDP that can be utilized in conjunction with the formal annual IDP process.

The most recent review has not been conducted for Whitney McDonald as she has left this lab.